Analyst

PAPER

View Article Online
View Journal | View Issue

Cite this: *Analyst*, 2024, **149**, 4487

Low-cost heat assisted ambient ionization source for mass spectrometry in food and pharmaceutical screening†

Odhisea Gazeli, ‡[a,b,f] Efstathios A. Elia, *‡[c] Nikolaos Argirusis,[d] Constantinos Lazarou,[a,b] Charalambos Anastassiou,[a,b] Joachim Franzke, [e] Juan F. Garcia-Reyes, [f] George E. Georghiou[a,b] and Agapios Agapiou[c]

Ambient Ionization Mass Spectrometry (AI-MS) techniques have revolutionized analytical chemistry by enabling rapid analysis of samples under atmospheric conditions with minimal to no preparation. In this study, the optimization of a cold atmospheric plasma for the analysis of food and pharmaceutical samples, liquid and solid, using a Heat-Assisted Dielectric Barrier Discharge Ionization (HA-DBDI) source is described. A significant enhancement in analyte signals was observed when a heating element was introduced into the design, potentially allowing for greater sensitivity. Furthermore, the synergy between the inlet temperature of the mass spectrometer and the heating element allows for precise control over the analytical process, leading to improved detection sensitivity and selectivity. Incorporating computational fluid dynamic (CFD) simulations into the study elucidated how heating modifications can influence gas transport properties, thereby facilitating enhanced analyte detection and increased signal intensity. These findings advance the understanding of HA-DBDI technology and provide valuable insights for optimizing AI-MS methodologies for a wide range of applications in food and pharmaceutical analysis.

Received 26th June 2024,
Accepted 18th July 2024

DOI: 10.1039/d4an00901k

rsc.li/analyst

Introduction

The use of Mass Spectrometry (MS) is a central approach for many relevant applications, providing high precision in molecular weight determination, thereby facilitating the precise identification of substances within diverse matrices. Continuous advancements in MS instrumentation have significantly enhanced its accuracy and sensitivity,[1] while concurrent progress in desorption/ionization (DI) techniques/methods has revolutionized the detection capabilities across several analytes. From metabolites[2] to biomarkers[3] and drugs,[4] these developments have markedly improved the ability to screen and quantify compounds within complex sample matrices.

Commercially available methods for ionizing analytes from samples before MS analysis include, but are not limited to, ElectroSpray Ionization (ESI),[5] Matrix-Assisted Laser Desorption/Ionization (MALDI),[6] Direct Analysis in Real-Time (DART).[7] However, the instrumentation needed for these methods is usually relatively expensive, and in some cases, the sample preparation procedures for using these are delicate and time-consuming. For this reason, there has been ongoing research to develop new ionization methods that are cost-effective, efficient, and user-friendly while at the same time complementing the performance of the above commercial ionization methods.[8,9] Based on this vision, one promising advancement in the field of MS is the use of ambient ionization (AI-MS), which allows for direct analysis of samples without extensive sample preparation procedures.[10]

Plasma-based AI-MS methods have attracted attention given the simplicity, speed of analysis, low manufacturing cost, and high sensitivity they offer. Notable examples are the Low Temperature Plasma probe (LTP),[11] Dielectric Barrier Discharge Ionization (DBDI)[12] and Flexible Microtube Plasma (FμTP).[13] These AI-MS methods rely on the unique properties

[a]*PHAETHON Centre of Excellence for Intelligent, Efficient and Sustainable Energy Solutions, Nicosia 2109, Cyprus*
[b]*ENAL Electromagnetics and Novel Applications Lab, Department of Electrical and Computer Engineering, University of Cyprus, Nicosia 2109, Cyprus*
[c]*Department of Chemistry, University of Cyprus, P.O. Box 20537, Nicosia, 1678, Cyprus. E-mail: elia.efstathios-andreas@ucy.ac.cy*
[d]*4mat4nrg GmbH, 38678 Clausthal-Zellerfeld, Germany*
[e]*Leibniz-Institut für Analytische Wissenschaften – ISAS – e.V., Bunsen-Kirchhoff-Str. 11, 44139 Dortmund, Germany*
[f]*Analytical Chemistry Research Group, Department of Physical and Analytical Chemistry, University of Jaén, 23071 Jaén, Spain*
†Electronic supplementary information (ESI) available. See DOI: https://doi.org/10.1039/d4an00901k
‡Joint first authors.

of plasma (ability to produce ions, radicals, and atomic species[14]) to ionize analytes under ambient conditions,[15] thus eliminating the need for sample preparation, making them suitable for the detection of polar, non-polar and low to medium molecular mass analytes as well as thermally labile samples[16] directly from the sample. Furthermore, they have been already used for the detection of potential cancer biomarkers,[3] food safety testing,[17] and forensic analysis.[18] Although most of plasma-based AI-MS sources are not yet commercially available, significant effort has been made to understand most of their physical and chemical characteristics.

For example, the LTP probe creates an alternating electric field that produces a half-dielectric barrier discharge, allowing the plasma to interact directly with the sample without damaging it. Therefore, it can be used on a variety of surfaces and is capable of detecting small amounts of analytes (~pg), such as explosives[18] and drugs.[4,19] Additionally, it can be used in a real-time analysis scenario and has been shown to detect compounds found in skin, tablets and biological samples,[11] while also being able to detect chemical substances directly from aqueous solutions.[11]

On the other hand, DBDI differ from corona discharges (like atmospheric pressure chemical ionization) and half-DBDI as they form plasma within a space separated from the electrodes by a dielectric material. In this way, the generated plasma is formed uniformly while preventing contamination of the plasma due to the degradation of electrodes.[20] Given these characteristics of DBDI, plasma is produced at lower temperatures compared to traditional "electrode contact" discharges while are able to perform dissociation, excitation, and ionization. Therefore, DBDI are a versatile method for analytical chemistry applications and can be tuned for the detection of a wide range of analytes.[21]

Like the above two methods, FμTP is a relatively new ambient ionization method designed for use with mass spectrometers and ion mobility spectrometers (IMS). It has been shown to improve plasma stability and reliability. Compared to existing plasma-based ionization methods such as DBDI and LTP, it exhibits superior performance in terms of sensitivity, ionization efficiency, and detection limit (especially for perfluoroalkanes – PFAs). It also shows a lower spectrum/plasma background and has been used to detect a variety of analytes such as ketones, low polar biomarkers and foods.[13,22–24]

In addition to the above methods, others with similar characteristics have been presented in the literature. For example, Bregy *et al.*[25] presented a new concept for real-time breath analysis. This new AI-MS method was also plasma-based and allowed researchers to perform online analysis for rapid and non-invasive medical diagnosis/monitoring through the detection of volatile organic compounds (VOCs) in breath. The AI-MS method was cost-effective (~€500), small in size and easy to use, while the researchers identified more than 100 VOCs in the human breath which could be used to monitor metabolic changes, such as those that occur after a meal.

The above methods demonstrate the important role of plasma-based AI-MS methods in advancing different mass spectrometry application areas. However, universal use has been limited by several factors. For example, commercially available plasma sources usually require expensive high-voltage (HV) power supplies, leading to high costs for a laboratory. In addition, plasma reactors require specialized personnel for their construction, which can complicate the development of such sources.

Based on this fact, Furter *et al.*[36] developed of a simple and low-cost DBDI source for use in AI-MS. The authors constructed the DBDI source using a double dielectric barrier discharge plasma cell embedded in epoxy resin. The plasma cell consisted of a fused silica tube with isolated ring electrodes positioned axially on the outside of the silica tube. The plasma was generated by applying a high voltage AC waveform from a resonant Royer oscillator circuit powered by a lab-built DC supply. Characterization of the plasma showed gas temperatures around room temperature and vibrational temperatures ranging from ~4000–8000 K depending on operating parameters. Species generated in the plasma include N_2, N_2^+, He, OH, H, and O. The DBDI source was used to directly analyze a variety of pharmaceuticals, illegal drugs, and food/flavoring samples with little fragmentation observed. Both qualitative and quantitative analysis was demonstrated, with quantitative analysis showing good linearity and detection limits in the low micromolar range. Given its simple and low-cost design using readily available components, this DBDI source provides an accessible option for small laboratories to add ambient ionization capabilities to existing mass spectrometers without requiring a commercially available product.

According to literature and our knowledge, the two most economically feasible plasma-based AI-MS methods have been studied by Bregy *et al.*[25] and Yang *et al.*[26] In the first study, the cost reduction was achieved using an audio amplifier as a power supply, while in the second, a custom glass plasma reactor for interfacing with the MS instrument was designed. While this reactor was an efficient approach, it poses challenges for users without access to a glass workshop. Additionally, Yang *et al.*[26] lowered the cost of the power supply by creating a home circuit board requiring electronics expertise that may not be practical or feasible for many end users. While these methods offer considerable cost savings and ease of use, they do rely on technical skills that could restrict wider adoption among analytical chemistry labs. Hence, further innovations are still necessary to ensure accessibility across all levels of expertise within this field.

The present manuscript describes an easy-to-build, low-cost and user-friendly plasma AI-MS method that can be constructed without specialized knowledge in circuit design or access to special workshops. This AI-MS method has been called Heat Assisted Dielectric Barrier Discharge Ionization (HA-DBDI), and as an initial demonstration of its capabilities, analytes commonly found in foods and pharmaceuticals were tested. Furthermore, computer simulations for the gas flow and the heat transfer (HT) were performed to better understand the physical characteristics and analytical performance of this source.

Experimental section

Parameter of mass spectrometer

An Agilent Single Quadrupole LC/MSD (model G6125B) was used to analyze all samples. To achieve efficient desorption and ionization of analytes, the instrument was operated under the following conditions: inlet temperature 250 °C, drying gas flow rate 12 L min^{-1}, nebulizer gas pressure 0 psig, quadrupole temperature 100 °C, capillary voltage 0 V.

Data processing. Obtained mass spectra in the proprietary .D format (MassHunter) were imported into OpenChrome® (LABLICATE) and exported as standard CSV files. These were then imported into OriginLabPro (2023b) for graphical representation and visualization.

Design and development of HA-DBDI source

A schematic representation of the HA-DBDI setup is illustrated in Fig. 1. The plasma reactor was built using a Volac borosilicate glass pipette of 150 mm and a UK 3-pin power plug. The flow rate of the gas feed (Helium 5.0, KIMGAS Industrial and Medical Gases Ltd) was 0.5 standard litres per minute (slm) and measured by a Bronkhorst MV flow meter (serial number M21213861A) and a range of 0.05–2 standard litres per minute. The glass pipette was chosen as a replaceable consumable part, and the UK plug was used as the base for the HV electrodes. By this approach, the position of the electrodes is fixed (twelve millimetres) ensuring consistent measurements and isolating HV components from the produced plasma and samples.

The solid samples were placed on a homemade 3D-printed base that can be adjusted on the MS system. Furthermore, samples were positioned 7.5 mm from the MS inlet and 8 mm from the pipette exit. Additionally, the pipette was placed perpendicular to the MS inlet. In order to measure the liquid samples, we used a cotton swab. The position of the cotton swab was the same as described for the solid samples.

The power supply diagram is shown in Fig. 2, and the costs of the components are presented in Table 1. This power supply can be readily constructed using parts that are accessible from local retailers and without requiring any additional programming skills. Moreover, it is capable of functioning with four different HV levels (18.8 kV, 24.4 kV, 26.3 kV, 33.8 kV), various frequencies (1 Hz–150 kHz), and an adaptable duty cycle (0%–100%). For this setup, it is important to ensure proper placement of the MOSFET IRFZ44, the HV transformer, and the resistor; these should be enclosed in a small container filled with standard or high-voltage transformer oil to maintain cool temperatures and prevent arcs within the secondary coil.

For the construction of the power supply, we acquired the high voltage transformer (serial number 054.0320) from a high frequency DC high voltage transformer kit and the frequency and duty cycle regulator (serial number 070.0329) from HELLAS Digital. It is important to note that although the transformer was purchased as part of a kit, only the transfor-

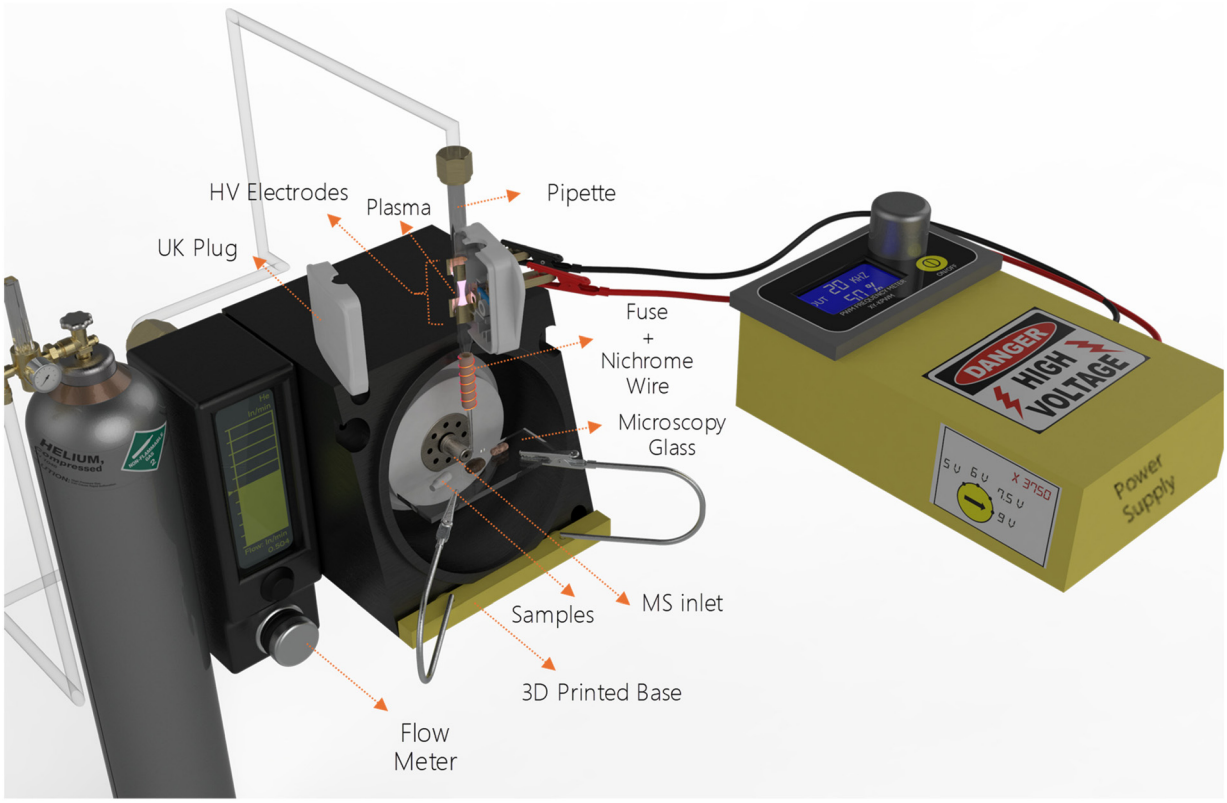

Fig. 1 Schematic representation of heat assisted dielectric barrier discharge ionization (HA-DBDI).

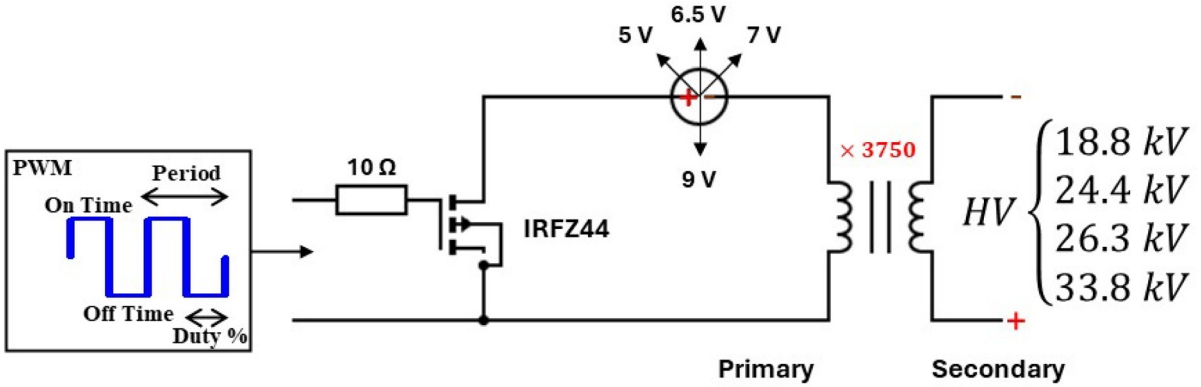

Fig. 2 Schematic diagram of the power supply of HA-DBDI.

Table 1 Cost evaluation of HA-DBDI source

Part name	Cost[a] (€)	Items
PWM module (1 Hz–150 kHz). Duty cycle adjustable	10	×1
3 V–12 V universal power supply 7.2 W	10	×2
15 kV high-frequency DC high voltage boost transformer (3.7 V DIY Kit)	4	×1
IRFZ44 TRANSISTOR N-FET 55 V 49 A 110 W	3	×1
10 Ω resistor 1 W	1.5	×1
Crocodile clips with cable	3	×1
3D printed case	5	×1
Transformer or a regular oil	~3	×1
Fuse	2	×1
Nichrome 80% 20% wire 22 gauge per meter	2	×1
Total	~55€	

[a] Prices were calculated based on our local retailers.

mer itself was used, and the remaining components from the kit were not utilized.

All components were assembled and housed inside a 3D-printed enclosure for space efficiency. In all experiments, a voltage of 9 V on the primary coil was used, resulting in a theoretical value of 33.8 kV output (on the secondary coil) at a frequency of 20 kHz and 50% duty cycle. Under these conditions, a stable and uniform plasma was formed within the central area between the HV electrodes inside the glass pipette.

The heater utilized in the HA-DBDI consisted of a porcelain fuse wrapped with nichrome wire containing 80% nickel and 20% chromium of 22-gauge thickness and resistance at 20 °C of 1.0118 [Ω ft^{-1}]. Six coil windings of the nichrome wire around the fuse, comprising approximately 264 millimetres in total length, were sufficient to generate a heated gas stream exiting the pipette tip at around 200 °C. Power was supplied to the heater using a standard laboratory power supply set to a fixed current of 5 A at 1.6 V. It should be noted that a deflection occurred in the part of the pipette near the heater area, which was attributed to high temperatures in this region. However, the user-friendly pipette exchange design helps mitigate this constraint by allowing for straightforward component replacement.

Chemicals and samples

For this study, unprocessed food samples and a pharmaceutical tablet that contained different substances were used. The food examination included 100% arabica coffee bean, low acidity olive oil, vanilla syrup, carob syrup and halloumi cheese. All the samples were obtained from the local market. The pharmaceutical tablet (Eladiet Good Night Melatonin) was also obtained from the local market. The tablet weighing 660 mg contained ingredients such as melatonin (1 mg), γ-aminobutyric acid (GABA) (100 mg), vitamin B3 (16 mg) and vitamin B6 (1.4 mg). Furthermore, a small pellet of bisphenol-A of 99.9% purity (Sigma Aldrich) was tested. The pellet was 3 mm in diameter and 3 mm in height and was prepared using a homemade pellet press.

Results and discussion

Preliminary study and optimization

The primary objectives of this study were threefold: (1) to assess the efficacy of atmospheric plasma in desorbing and ionizing analytes without enabling the HA-DBDI heating element, (2) to examine the influence of temperature on signal intensity, and (3) to determine the capability of the HA-DBDI to desorb and ionize analytes without enabling the plasma. Caffeine directly desorbed from a roasted coffee bean was used as a model sample to evaluate the analytical performance of the HA-DBDI at varying temperature conditions of the capillary inlet of the mass spectrometer. Caffeine is commonly used as a benchmark test compound for ambient ionization techniques due to its low molecular weight and ease of detection.[27]

Total ion currents (TICs) were obtained for the caffeine analyte at three different inlet temperatures of the mass spectrometer (100 °C, 200 °C, and 300 °C) while operating the HA-DBDI with the plasma activated alone and with both the plasma and heater of HA-DBDI engaged (Fig. 3). With the plasma deactivated for approximately 1–2 minutes, the independent and combined effects of the heating element could be observed. The findings revealed several notable results.

First, the HA-DBDI could be operated with or without the auxiliary heating element, whereas heating the working gas

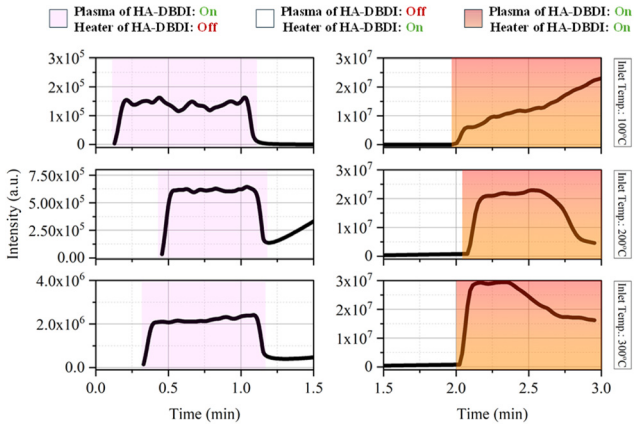

Fig. 3 Total ion currents (TICs) for three different temperatures of the MS capillary inlet and three distinct operational modes of HA-DBDI. The labels on the right side of the figure indicate the inlet temperatures of the MS, while the color-coded boxes at the top represent the three different operational modes of HA-DBDI. To facilitate a better comparison between the purple and orange operational modes of HA-DBDI signal intensities, the time axis is divided into two intervals.

flow alone was insufficient to generate caffeine ions. TIC increased substantially, from 2×10^5 to 2×10^6 arbitrary units, as the inlet temperature of the MS was raised from 100 °C to 300 °C with only the plasma of HA-DBDI activated (Fig. 3). This temperature dependence suggests that ion clustering plays an important role in HA-DBDI performance, with higher temperatures promoting cluster decomposition and boosting detectable ion signals (Fig. 4). Previous research has documented ion clustering under various desorption/ionization conditions.[28–30]

In contrast, the TIC remained stable at around 3×10^7 (arbitrary units) across all inlet temperatures when the HA-DBDI heater was co-activated with the plasma (Fig. 3). Thus, auxiliary heating likely suppresses cluster formation through energy transfer interactions at the sample surface, aided by the heated carrier gas stream of HA-DBDI and desorption processes at the sample surface. Finally, the TIC current decreased for inlet temperatures of 200 °C and 300 °C after two and a half minutes, attributed to heat deformation of the pipette glass by the HA-DBDI heater.

A closer look at the heating element of the HA-DBDI

The previous results demonstrated that applying thermal energy to the HA-DBDI enhances the signal intensity. Computational fluid dynamics (CFD) and heat transfer (HT) simulations were conducted using COMSOL Multiphysics 4.4 software to further investigate this phenomenon. Modelling CFD and HT mechanisms provides a deeper mechanistic understanding of this critical enhancement. For details on the modelling process, see the ESI.†

Specifically, a two-dimensional (2D) model was constructed focusing on the plane of symmetrical geometry encompassing

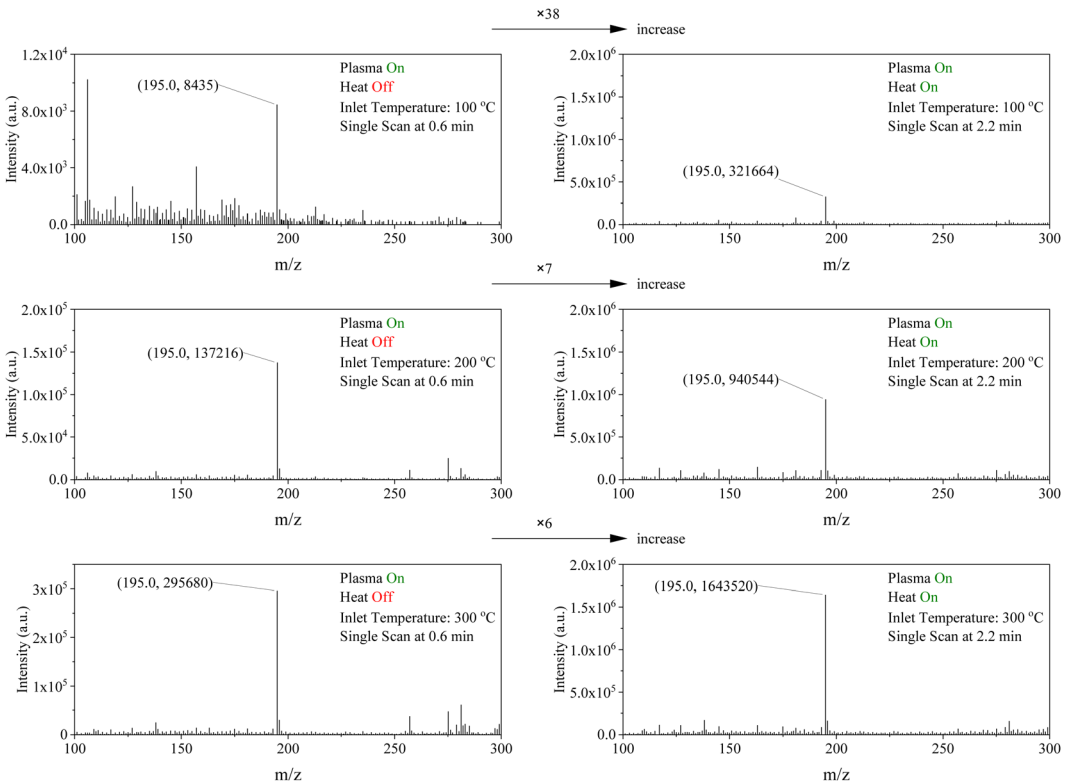

Fig. 4 Increase of caffeine signal (*m*/*z* 195) due to the activation of the heater of HA-DBDI for three different temperatures of the capillary inlet of the mass spectrometer.

the mass spectrometer inlet and HA-DBDI. Under these conditions, the governing equations employed for the flow dynamics were the Reynolds-Averaged Navier–Stokes (RANS) equations coupled with a standard k-ε turbulence model.[28]

This turbulence model was selected to account for irregular flow behaviour anticipated in the interaction zone between the helium carrier gas and the sample, while the equations above were solved under steady-state conditions. Furthermore, to simulate the behaviour of caffeine protonated molecules ($CF + H^+$) at the coffee surface, a time-dependent simulation was employed for a duration of 10 millisecond. Specifically, many $CF + H^+$ were initialized uniformly on the coffee bean surface. These protonated molecules were free to move, with zero initial velocity, under the influence of the CFD computed flow and pressure as well as HT computed temperature fields. For this simulation, it was hypothesized that such kinetic agitation would induce deviations from uniform distribution as molecules desorbed from the surface of the coffee bean. By tracing migrating molecules over simulated time, this computational approach aimed to model the transport of desorbed caffeine away from the solid interface into the fluid phase. While necessarily simplifying compared to experimental reality, such an arbitrarily assumed motion/simulation technique finds support from the experimental results presented above. These experiments showed that caffeine was desorbed in all cases, and as a result, this fact can be used in the simulation as a valid assumption.

The CFD/HT – $CF + H^+$ simulation effectively modelled the HA-DBDI ion source over a 10-millisecond period. In the ESI,†

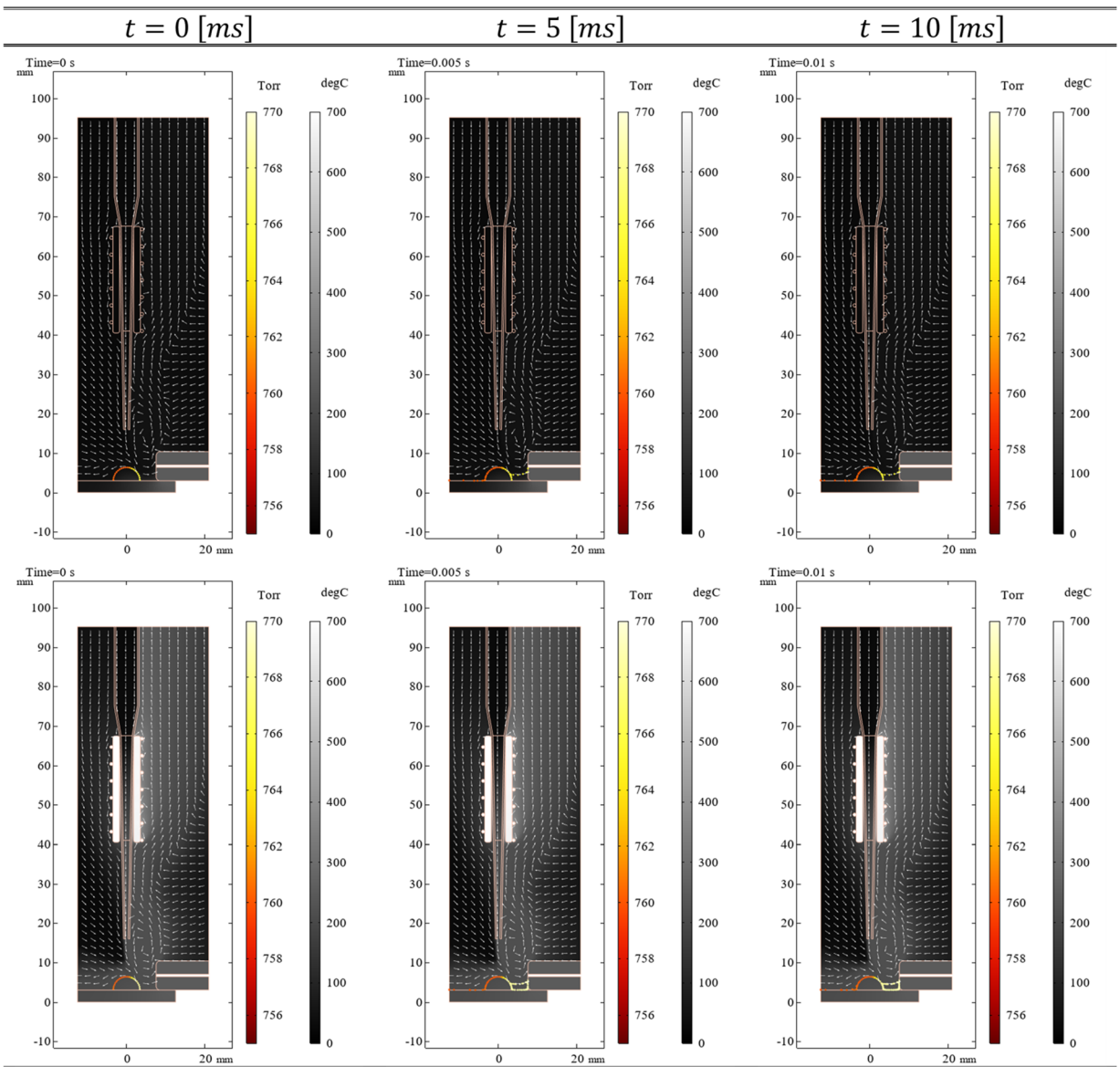

Fig. 5 Results of the simulation of the HA-DBDI source for three different time instances. On the top line, the HA-DBDI with the heater off is given, while on the bottom line, the HA-DBDI with the heater on is given. The pressure scale is given in Torr and the colour bar varies from red to yellow while the temperature scale is given in degrees of Celsius and the colour bar varies from black to white.

animations depicting the desorption of molecular caffeine ions under the influence of the flow dynamics and heat generated by the HA-DBDI are presented (refer to the files named "molecular_ion_animations_on.gif" & "molecular_ion_animations_off.gif"). Fig. 5 illustrates three snapshots of protonated caffeine, with and without the integrated heater of HA-DBDI. Each image includes colour bars on the right, representing simulated scalar fields of heat and pressure. The pressure field is superimposed directly onto the virtual protonated caffeine to elucidate its effect on analyte trajectories. Moreover, white arrows indicate the direction of helium gas flow, aiding comprehension of analyte species movement.

The results reveal that because of the vacuum of the MS inlet, the helium gas tends to move in the right side of the geometry and because of the expansion to the open boundaries, far from the MS inlet, transfers heat energy to the right part of the heater of HA-DBDI source. As a result, the temperature in the right part of the heater is higher than that in the left part. Furthermore, the gas flow dynamics remain largely consistent with or without the heater activated (as indicated by the direction of flow in Fig. 5), while the pressure near the inlet increases by ~3 torr when the heater is active (as indicated by the colour of the CF + H^+ depicted as circles in Fig. 5). This observation suggests that the pressure exerted on the surface of the coffee bean is a key physical mechanism influencing the

Table 2 Selected compounds interrogated with the proposed low-cost HA-DBDI source

Analyte name	Formula	Polarity	Detected ion [*m*/*z*]
6-Methyl-3-pyridinol	C_6H_7NO	$[M + H]^+$	110.1
3-Ethyl-2-hydroxy-2-cyclopenten-1-one	$C_7H_{10}O_2$	$[M + H]^+$	127.0
4-Vinylguaiacol	$C_9H_{10}O_2$	$[M + H]^+$	151.1
Caffeine	$C_8H_{10}N_4O_2$	$[M + H]^+$	195.0
Cholesterol	$C_{27}H_{46}O$	$[M - H_2O + H]^+$	369.2
GABA	$C_4H_9NO_2$	$[M + H]^+$	104.1
Vaniline	$C_8H_8O_3$	$[M + H]^+$	153.1
Melatonin	$C_{13}H_{16}N_2O_2$	$[M + H]^+$	233.1
Vitamin B3	C_5H_4NCOOH	$[M + H]^+$	124.0
Vitamin B6	$C_8H_{11}NO_3$	$[M + H]^+$	170.2
Bisphenol A	$C_{15}H_{16}O_2$	$[M - H]^-$	227.0
Caffeic acid	$C_9H_8O_4$	$[M - H]^-$	179.0
Ferulic acid	$C_{10}H_{10}O_4$	$[M - H]^-$	193.0
Oleic acid	$C_{18}H_{34}O_2$	$[M - H]^-$	281.2

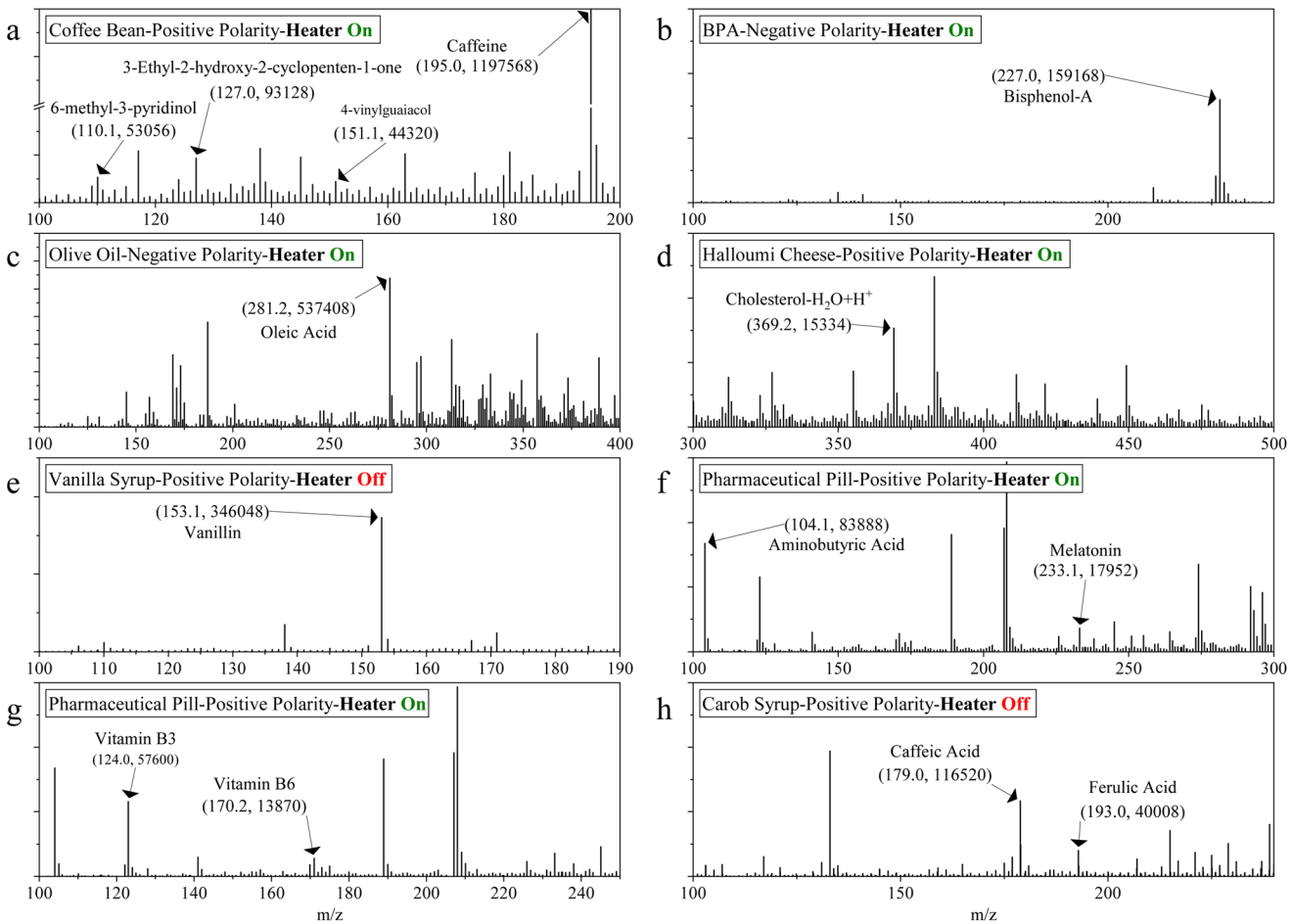

Fig. 6 Screening of different samples with HA-DBDI. (a) Coffee bean sample, (b) bisphenol A, (c) olive oil sample, (d) halloumi cheese sample, (e) vanilla syrup sample, (f) and (g) pill sample, (h) carob syrup sample.

behaviour of desorption of caffeine near the inlet. Consequently, when the heater is active, the desorption of caffeine is intensified and the number of particles in front of the inlet multiplies compared to when it is inactive. These findings, along with the assumption of clusters discussed in the previous section, offer a plausible complementary explanation for the heightened signal intensity observed when the heater of HA-DBDI is enabled.

Screening of selected analytes

A clear picture of the physical characteristics of HA-DBDI was established as proof of concept, and a variety of analytes in different samples were detected. Table 2 summarizes the analytes detected with HA-DBDI in various samples while in Fig. 6 the mass spectra are given.

For the coffee bean analysis two key components, caffeine and certain aromatic compounds, were detected through direct analysis *via* HA-DBDI. Similar, bisphenol-A was readily identifiable in the pellet sample. In contrast, analysis of the carob syrup revealed two common acids native to the carob fruit:[31] caffeic acid and ferulic acid.[32] Olive oil and halloumi cheese samples were found to contain oleic acid[33] and cholesterol,[24] respectively – two analytes typically abundant in these food matrices. However, the olive oil spectrum exhibited notable noise, which could stem from the thermal stability of olive oil[34] impacting desorption efficiency during analysis. Further experimental work is needed to elucidate better the effects of varying sample properties on plasma–sample interactions under ambient conditions.

The vanilla syrup spectrum was free of any background interferences from matrix or plasma. Interestingly, both the carob syrup and vanilla samples displayed diminishing analyte signal intensity upon enabling the HA-DBDI heater, likely because the presence of water in these samples impacts the ionization efficiency of ambient plasma sources, as water is known to influence the plasma ionization processes.[35–37]

Analysis of the tablet sample enabled the identification of nearly all compounds listed on the product packaging. Notably, peaks at *m*/*z* 124.0 and 170.2 were tentatively assigned as vitamins B3 and B6, respectively. A comparison of relative peak intensities revealed that vitamin B3 levels exceeded those of vitamin B6, corroborating information provided on the label specifying a distinctly higher concentration of B3. This could be attributed to multiple factors including increased ionisation efficiency for vitamin B3 compared to vitamin B6, a difference in the sensitivity response of the two analytes, or simply the difference in the relative abundance of these vitamins in the tablet. Additionally, the presence of aminobutyric acid and melatonin within the sample was observed, which was consistent with the labelling specifications.

Conclusions

This study successfully demonstrates the efficacy of the HA-DBDI source for analysing caffeine and other compounds in various samples, including foods and pharmaceuticals. By integrating a heating element within the DBDI source, the analytical performance is significantly enhanced, while computational fluid dynamics modelling provides insights into how heat alters gas transport properties. The HA-DBDI method proves to be a powerful tool for screening a wide range of analytes without prior sample preparation, allowing for the detection of even low concentrations of VOCs. Furthermore, the impact of heat on desorption efficiency is sample-dependent, with challenging samples like olive oil due to their heat resistance, while the presence of water in samples like syrup interferes with ionization efficiency. The HA-DBDI source allows the detection of relevant compounds within complex matrices, reflecting its potential usefulness for various analytical applications in fields such as food safety and pharmaceutical quality control. In conclusion, this method can substantially improve the sensitivity and efficiency of ion detection, making it a valuable addition to the toolbox of analytical techniques for both research and practical uses across diverse sectors of analytical chemistry.

Author contributions

All authors contributed equally.

Data availability

The data supporting this article have been included as part of the ESI.†

Conflicts of interest

Authors declare no conflict of interest.

Acknowledgements

This project has received funding from the European Union's Horizon 2020 research and innovation program under grant agreement 810686. E. A. E. received funding from the European Union under Marie Skłodowska-Curie Actions (grant no. 101109014).

References

1 C. D. Chouinard, *J. Mass Spectrom. Adv. Clin. Lab*, 2022, **26**, 21–22.
2 E. A. Elia, M. Niehaus, R. T. Steven, J.-C. Wolf and J. Bunch, *Anal. Chem.*, 2020, **92**, 15285–15290.
3 P. Vogel, C. Lazarou, O. Gazeli, S. Brandt, J. Franzke and D. Moreno-González, *Anal. Chem.*, 2020, **92**, 9722–9729.
4 A. U. Jackson, J. F. Garcia-Reyes, J. D. Harper, J. S. Wiley, A. Molina-Díaz, Z. Ouyang and R. Graham Cooks, *Analyst*, 2010, **135**, 927.

5 S. Chen, J. Zeng, Z. Zhang, B. Xu and B. Zhang, *J. Chromatogr. Open*, 2022, **2**, 100064.
6 V. M. Doroshenko, V. V. Laiko, N. I. Taranenko, V. D. Berkout and H. S. Lee, *Int. J. Mass Spectrom.*, 2002, **221**, 39–58.
7 J. H. Gross, *Anal. Bioanal. Chem.*, 2014, **406**, 63–80.
8 C. L. Feider, A. Krieger, R. J. DeHoog and L. S. Eberlin, *Anal. Chem.*, 2019, **91**, 4266–4290.
9 G. A. Harris, L. Nyadong and F. M. Fernandez, *Analyst*, 2008, **133**, 1297.
10 M.-Z. Huang, S.-C. Cheng, Y.-T. Cho and J. Shiea, *Anal. Chim. Acta*, 2011, **702**, 1–15.
11 J. D. Harper, N. A. Charipar, C. C. Mulligan, X. Zhang, R. G. Cooks and Z. Ouyang, *Anal. Chem.*, 2008, **80**, 9097–9104.
12 C. Meyer, S. Müller, E. L. Gurevich and J. Franzke, *Analyst*, 2011, **136**, 2427.
13 S. Brandt, F. D. Klute, A. Schütz, U. Marggraf, C. Drees, P. Vogel, W. Vautz and J. Franzke, *Anal. Chem.*, 2018, **90**, 10111–10116.
14 S. Reuter, T. von Woedtke and K.-D. Weltmann, *J. Phys. D: Appl. Phys.*, 2018, **51**, 233001.
15 M. Aida, T. Iwai, Y. Okamoto, S. Kohno, K. Kakegawa, H. Miyahara, Y. Seto and A. Okino, *Mass Spectrom.*, 2017, **6**, S0075–S0075.
16 A. Albert and C. Engelhard, *Anal. Chem.*, 2012, **84**, 10657–10664.
17 J. S. Wiley, J. F. García-Reyes, J. D. Harper, N. A. Charipar, Z. Ouyang and R. G. Cooks, *Analyst*, 2010, **135**, 971.
18 Y. Zhang, X. Ma, S. Zhang, C. Yang, Z. Ouyang and X. Zhang, *Analyst*, 2009, **134**, 176–181.
19 D. N. Ateacha, C. Kuhlmann and C. Engelhard, *Anal. Methods*, 2019, **11**, 566–574.
20 M. Cogollo de Cádiz, A. López Arrabal, A. Díaz Lantada and M. V. Aguirre, *Sci. Rep.*, 2021, **11**, 24175.
21 S. Brandt, F. D. Klute, A. Schütz and J. Franzke, *Anal. Chim. Acta*, 2017, **951**, 16–31.
22 C. Drees, A. Schütz, G. Niu, J. Franzke, W. Vautz and S. Brandt, *Anal. Chim. Acta*, 2020, **1127**, 89–97.
23 A. Knodel, D. Foest, S. Brandt, N. Ahlmann, U. Marggraf, B. Gilbert-López and J. Franzke, *Anal. Chem.*, 2020, **92**, 15212–15220.
24 D. Foest, A. Knodel, S. Brandt and J. Franzke, *Anal. Chim. Acta*, 2022, **1201**, 339619.
25 L. Bregy, P. M.-L. Sinues, M. M. Nudnova and R. Zenobi, *J. Breath Res.*, 2014, **8**, 027102.
26 C.-C. Yang and C.-H. Lin, *Comput. Electr. Eng.*, 2016, **54**, 210–216.
27 D. Brecht, F. Uteschil and O. J. Schmitz, *Rapid Commun. Mass Spectrom.*, 2021, **35**(10), e9071.
28 M. Niehaus, K. N. Robinson, T. Murta, E. A. Elia, A. M. Race, B. Yan, R. T. Steven and J. Bunch, *J. Am. Soc. Mass Spectrom.*, 2020, **31**, 2287–2295.
29 B. A. Thomson, *J. Am. Soc. Mass Spectrom.*, 1997, **8**, 1053–1058.
30 S. Klee, V. Derpmann, W. Wißdorf, S. Klopotowski, H. Kersten, K. J. Brockmann, T. Benter, S. Albrecht, A. P. Bruins, F. Dousty, T. J. Kauppila, R. Kostiainen, R. O'Brien, D. B. Robb and J. A. Syage, *J. Am. Soc. Mass Spectrom.*, 2014, **25**, 1310–1321.
31 B. E. Launder and D. B. Spalding, *Comput. Methods Appl. Mech. Eng.*, 1974, **3**, 269–289.
32 J.-K. Moon and T. Shibamoto, *J. Agric. Food Chem.*, 2009, **57**, 5823–5831.
33 V. Goulas, E. Stylos, M. Chatziathanasiadou, T. Mavromoustakos and A. Tzakos, *Int. J. Mol. Sci.*, 2016, **17**, 1875.
34 L. B. Roseiro, L. C. Duarte, D. L. Oliveira, R. Roque, M. G. Bernardo-Gil, A. I. Martins, C. Sepúlveda, J. Almeida, M. Meireles, F. M. Gírio and A. P. Rauter, *Ind. Crops Prod.*, 2013, **47**, 132–138.
35 J. F. García-Reyes, F. Mazzoti, J. D. Harper, N. A. Charipar, S. Oradu, Z. Ouyang, G. Sindona and R. G. Cooks, *Rapid Commun. Mass Spectrom.*, 2009, **23**, 3057–3062.
36 J. S. Furter and P. C. Hauser, *Anal. Methods*, 2018, **10**, 2701–2711.
37 G. A. Newsome, L. K. Ackerman and K. J. Johnson, *J. Am. Soc. Mass Spectrom.*, 2016, **27**, 135–143.